Anti-tubercular activity of novel 4-anilinoquinolines and 4-anilinoquinazolines

Christopher R. M. Asquith[a,b], **Neil Fleck**[c], **Chad D. Torrice**[d], **Daniel J. Crona**[d,e], **Christoph Grundner**[c,f,*], **William J. Zuercher**[b,e,*]

[a]Department of Pharmacology, School of Medicine, University of North Carolina at Chapel Hill, Chapel Hill, NC 27599, USA

[b]Structural Genomics Consortium, UNC Eshelman School of Pharmacy, University of North Carolina at Chapel Hill, Chapel Hill, NC 27599, USA

[c]Seattle Children's Research Institute, Seattle, WA 98101, USA

[d]Division of Pharmacotherapy and Experimental Therapeutics, UNC Eshelman School of Pharmacy, University of North Carolina at Chapel Hill, Chapel Hill, NC 27599, USA

[e]Lineberger Comprehensive Cancer Center, University of North Carolina at Chapel Hill, Chapel Hill, NC 27599, USA

[f]Department of Global Health, University of Washington, Seattle, WA 98195, USA

Abstract

We screened a series of 4-anilinoquinolines and 4-anilinoquinazolines and identified novel inhibitors of *Mycobacterium tuberculosis (Mtb)*. The focused 4-anilinoquinoline/quinazoline scaffold arrays yielded compounds with high potency and the identification of 6,7-dimethoxy-*N*-(4-((4-methylbenzyl)oxy)phenyl)quinolin-4-amine (**34**) with an MIC_{90} value of 0.63-1.25 μM. We also defined a series of key structural features, including the benzyloxy aniline and the 6,7-dimethoxy quinoline ring, that are important for *Mtb* inhibition. Importantly the compounds showed very limited toxicity and scope for further improvement by iterative medicinal chemistry.

Graphical Abstract
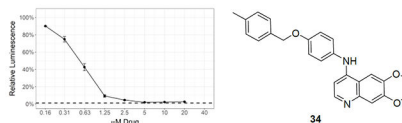
Keywords

Anti-tubercular; 4-anilinoquinoline; 4-anilinoquinazoline; *Mycobacterium tuberculosis (Mtb)*

Mycobacterium tuberculosis (Mtb), the causative agent of tuberculosis (TB) in humans,[1] infects nearly a third of the earth's population and caused 1.6 million worldwide deaths in 2017.[2] With nearly ten million new cases of active disease each year, TB is now the leading cause of death from infectious disease globally.[2] Current therapeutic strategies involve the use of a combination of anti-microbial agents including ethambutol, isoniazid, pyrazinamide and rifampicin (Fig. 1).[3] However, more than 5% of *Mtb* infections now involve multidrug-resistant (MDR-TB) and extensively drug-resistant (XDR-TB) *Mtb* strains. MDR-TB is associated with a 50% mortality rate whereas XDR-TB is nearly always fatal.[4] There is an urgent need for new therapeutic strategies.

Human protein kinases are pharmacologically tractable enzymes targeted by more than three dozen approved medicines.[5] Hundreds of additional kinase inhibitors are under clinical and preclinical investigation. There is growing recognition that pathogen kinases may be targeted in the treatment of infectious diseases.[6–7] Considering the conserved ATP-binding site across species, we looked to screen collections of ATP-competitive inhibitors of human kinases for their anti-tubercular activity.

To identify new chemical starting points against *Mtb* we looked to lapatinib, gefitinib, and erlotinib as starting points which have recently been revealed to have activity against *Mtb* (Fig. 2.).[5],[8] We tested the activity of lapatinib, gefitinib, and erlotinib against *Mtb* by measuring luminescence and growth on solid medium across a series of four two-fold dilutions starting at 20 μM (Tab 1).[9–10] The reduction of visible growth on solid medium demonstrated the compounds to be bactericidal.

Gefitinib treatment had no effect relative to the absence of compound. Erlotinib induced a modest effect that appeared to plateau at a signal of approximately 70 %. In contrast, lapatinib showed activity even at 5 μM and reduced the relative *Mtb* signal to below 10 % at 20 μM. This result suggested that the 4-benzyloxy aniline substituent might be important for anti-*Mtb* activity. These compounds demonstrate only limited toxicity in a human skin fibroblast cell line (WS-1) counter screen.[11]

To further explore quinazoline *Mtb* activity, we profiled several focused arrays of compounds to probe the structure activity relationships of the quinoline/quinazoline. We hence synthesized a series of compounds (**1-34**) following up on the results listed in table 1, exploring the 4-anilinoquinoline and 4-anilinoquinazoline scaffolds through nucleophilic aromatic displacement of 4-chloroquin(az)olines. (Sch. 1) We were able to access products in good to excellent yields (55-91 %) consistent with previous reports and without protection of the alcohol substituted quin(az)oline starting material.[11–13]

The first set of compounds probed a replacement of the 6-postion morpholine segment of gefitinib with a simple alcohol on the lapatinib scaffold (Tab. 2).[14] Although neither the 6-OH (**1**) or 7-OH (**2**) quinazoline showed appreciable activity, the 6,7-dihydroxy compound (**3**) began to inhibit *Mtb* growth at higher concentrations. The analogous set of methoxy-substituted compounds (**4-6**) had very similar activity profiles. The 6-OH quinoline (**7**) showed improved activity relative to the matched quinazoline (**1**). The inclusion of fluorine substitution on the phenyl ring distal to the quinazoline (**8-10**) led to markedly increased

activity for all three isomers. At 20 μM, **8-10** all reduced the relative *Mtb* signal to 25-37 %, and a modest but discernable reduction in signal was observed at 1.25 μM. Interestingly, the effect of fluorine substitution led to a different activity pattern from changing quinazoline ring substitution as the modification of **1** to the 7-OH (**11**) or 6,7-(OH)$_2$ (**12**) resulted in a significant loss of activity, even at 20 μM. These results demonstrated that *Mtb* activity was sensitive to changes at multiple parts of the template and that these changes were not necessarily additive. We counter screened **1-12** in human skin fibroblast cells (WS-1) and observed very limited toxicity with **3** and **7** the only compounds in the single digit micromolar range (IC$_{50}$ = 8.8 and 2.5 μM respectively).[15]

The next set of quin(az)olines profiled was prepared to explore the contributions from both the aniline and the core heterocycle (Tab. 3).[11,16] The larger 3,4,5-trimethoxyphenyl aniline was employed on several diversely substituted quinolines and quinazolines (**13-18**) which led to no observable activity except when paired with the 6,7-(OCH$_2$CH$_2$OMe)$_2$-quinazoline of erlotinib (**19**) which had only slight activity at 20 μM. On the other hand, incorporation of the aniline fragment from erlotinib (3-ethynylphenyl) did yield several active compounds, including the quinoline analog of erlotinib (**20**). The erlotinib aniline with a 6,7-(OMe)$_2$-substituted quinoline core (**21**) or quinazoline (**22**) showed activity but not with the 3-cyanoquinoline (**23**). The analogous 3-bromophenyl aniline compounds (**24-26**) showed higher activity than the paired 3-ethynylphenyl compounds. Finally, the aniline substitution from lapatinib (3-Cl-4-(2-F-PhO)Ph) yielded a marginally active quinazoline (**27**) and a highly active quinoline (**28**) that had 10 % *Mtb* signal at 20 μM. We counter screened **13-28** in WS-1 cells and observed limited toxicity in most compounds. However, the bromine substitution appeared to increase toxicity (**24-26**) along with the lapatinib derivatives (**27-28**).

A subsequent set of compounds explored features of the 4-benzyloxyaniline portion of the quinoline template (Tab. 4).[17–18] Variation of the ether linkage to an amide and addition of a hydroxy on the aniline portion revealed an activity pattern where 6,7-dimethoxy substitution with the benzylic arm was active (**29-30**). In contrast, truncation of the benzyl also removed the activity as in acetamide **31**, which had no effect on*Mtb*. The 6-methoxy (**32**) and 7-methoxy (**33**) showed no reduction in *Mtb* signal at 20 μM. However, switching back to the 4-methyl benzyl ether linked compound **34** yielded the most potent activity observed with any compound in the present study, with a robust signal observed even at 1.25 μM. The *Mtb* MIC$_{90}$ for **34** was in the 0.63-1.25 μM range. However, the kill curve plateaued at 5 μM, and no improved killing was observed at higher doses (98 % inhibition at 5 μM; 98 % inhibition at 20 μM) (Fig. 3).

As with the other compound sets, we evaluated **29-34** in human skin fibroblast cells (WS-1) and observed moderate toxicity in the single digit micromolar range for most compounds.[18] Importantly, the anti-*Mtb* effects of compounds appeared to be divergent from the toxic effects in WS-1 cells, suggesting that the *Mtb* effects were not driven by nonspecific cytotoxicity. The most potent anti-*Mtb* compound **34** had WS-1 IC$_{50}$ = 5.4 μM, substantially higher than its *Mtb* MIC$_{90}$ value and within threefold of the IC$_{50}$ values for erlotinib and lapatinib. This result demonstrated that, in the human WS-1 cell line, **34** behaved comparably to two approved medicines.

These structure activity relationships between *Mtb* activity and the 4-anilinoquinoline/ quinazoline scaffold have the potential to inform a medicinal chemistry strategy for enhanced *Mtb* activity. The most sensitive structural changes were found to be in the ring appended to the aniline rather than in the quin(az)oline core.

This body of work provides a number of exciting starting points for further optimization, with limited non-specific toxicity. However, the failure to achieve complete parasite kill led us to deprioritize the series due to the potential for resistance to develop. The mechanism of anti-*Mtb* activity of the quin(az)olines has yet to be defined. These compounds were originally prepared as inhibitors of human kinases targeting the ATP-binding site, a rational starting hypothesis for the mechanism of action is that the effects of these compounds are mediated by inhibition of *Mtb* kinases. However, it is possible that the observed phenotypes may originate from modulation of other, non-kinase ATP-binding proteins in the organism.

Gefitinib, erlotinib, and lapatinib have previously been reported to inhibit the intracellular growth of *Mtb*. Multiple lines of evidence were described suggesting inhibition of the host target epidermal growth factor receptor (EGFR) was responsible for this activity.[15] However our results demonstrate that proteins within the pathogen itself may be targeted as well. The benzyl substituent present in the molecule showed a pivotal effect to potency, as is highlighted by the enhanced activity of **34** relative to **30**. The present results help define a de-risked medicinal chemistry trajectory towards anti-tubercular compounds with targets in both the host and the parasite itself. Such dual acting compounds might offer advantages in efficacy and/or reduction in propensity for resistance.

Supplementary Material

Refer to Web version on PubMed Central for supplementary material.

Acknowledgments

References and notes

1. Pai M; Behr MA; Dowdy D; Dheda K; Divangahi M; Boehme CC; Ginsberg A; Swaminathan S; Spigelman M; Getahun H; Menzies D; Raviglione M Nat Rev Dis Primers 2016, 2, 16076. [PubMed: 27784885]

2. World Health Organization. Global Tuberculosis Report 2018 (WHO, 2018).

3. Chan ED; Iseman MD BMJ. 2002, 325, 1282. [PubMed: 12458250]

4. Floyd K; Glaziou P; Zumla A; Raviglione M Lancet Respir Med 2018, 6, 299. [PubMed: 29595511]

5. Ferguson FM; Gray NS Nat Rev Drug Discov. 2018, 17, 353. [PubMed: 29545548]

6. Sachan M; Srivastava A; Ranjan R; Gupta A; Pandya S; Misra A Curr Pharm Des. 2016, 22, 2599. [PubMed: 26818871]

7. Glennon EKK; Dankwa S; Smith JD; Kaushansky A Trends Parasitol. 2018, 34, 843. [PubMed: 30122551]

8. Stanley SA; Barczak AK; Silvis MR; Luo SS; Sogi K; Vokes M; Bray MA; Carpenter AE; Moore CB; Siddiqi N; Rubin EJ; Hung DT PLoS Pathog. 2014, 10, e1003946. [PubMed: 24586159]

9. Andreu N; Fletcher T; Krishnan N; Wiles S; Robertson BD J Antimicrob Chemother. 2012, 67, 404. [PubMed: 22101217]

10. An H37Rv strain containing an auto-luminescence operon (LuxABCDE) was grown to log phase, diluted and re-grown for at least 2 doublings to a final OD_{600} of 0.005. Cultures were dispensed into 96-well white, flat-bottom plates in 100 μL final volume. Luminescence was quantified using a PHERTAstar plate reader (BMG Labtech) blanked against 7H9 media.

11. Asquith CRM; Naegeli KM; East MP; Laitinen T; Havener TM; Wells CI; Johnson GL; Drewry DH; Zuercher WJ; Morris DC J Med Chem. 2019, 62, 4772. [PubMed: 30973735]

12. Asquith CRM; Laitinen T; Bennett JM; Godoi PH; East MP; Tizzard GJ; Graves LM; Johnson GL; Dornsife RE; Wells CI; Elkins JM; Willson TM; Zuercher WJ ChemMedChem 2018, 13, 48. [PubMed: 29072804]

13. Asquith CRM; Treiber DK; Zuercher WJ Bioorg Med Chem Lett. 2019, 29, 1727. [PubMed: 31129055]

14. **General procedure for the synthesis of 4-anilinoquin(az)olines**: 4-chloroquin(az)oline derivative (1.0 eq.), aniline derivative (1.1 eq.), and ^{i}Pr$_2$Net (2.5 eq.) were suspended in ethanol (10 mL) and refluxed for 18 h. The crude mixture was purified by flash chromatography using EtOAc:hexane followed by 1-5 % methanol in EtOAc; After solvent removal under reduced pressure, the product was obtained as a free following solid or recrystallized from ethanol/water.**4-{[4-(benzyloxy)phenyl]amino}quinazolin-6-ol** (**1**) as a yellow solid (68 %, 220 mg, 0.640 mmol) MP 231-233 °C; ^{1}H NMR (400 MHz, DMSO-d_6) δ 11.21 (s, 1H), 10.91 (s, 1H), 8.75 (s, 1H), 8.04 (d, *J* = 2.5 Hz, 1H), 7.88 (d, *J* = 9.0 Hz, 1H), 7.70 (dd, *J* = 9.1, 2.5 Hz, 1H), 7.62 – 7.57 (m, 2H), 7.52 – 7.44 (m, 2H), 7.44 – 7.37 (m, 2H), 7.37 – 7.30 (m, 1H), 7.14 – 7.09 (m, 2H), 5.16 (s, 2H). ^{13}C NMR (101 MHz, DMSO-d_6) δ 158.8, 157.8, 156.7, 148.1, 136.9, 131.6, 129.7, 128.5 (2C, s), 127.9, 127.7 (2C, s), 126.5, 126.2 (2C, s), 121.2, 114.92, 114.85 (2C, s), 107.1, 69.4. HRMS m/z [M+H]$^+$ calcd for $C_{21}H_{18}N_3O_2$: 344.1399 found = 344.1386; LC t_R = 4.24 min, >98% Purity.**4-{[4-(benzyloxy)phenyl]amino}quinazolin-7-ol** (**2**) as a light yellow solid (78 %, 223 mg, 0.648 mmol) MP 277-279 °C; ^{1}H NMR (400 MHz, DMSO-d_6) δ 11.76 (s, 1H), 11.42 (s, 1H), 8.76 (d, *J* = 9.0Hz, 1H), 8.74 (s, 1H), 7.59 – 7.54 (m, 2H), 7.49 – 7.44 (m, 2H), 7.42 – 7.38 (m, 2H), 7.36 – 7.28 (m, 3H), 7.12 – 7.07 (m, 2H), 5.15 (s, 2H). ^{13}C NMR(101 MHz, DMSO-d_6) δ 164.3, 158.9, 156.6, 150.5, 140.4, 136.9, 129.7, 128.5 (2C, s), 127.9, 127.7 (2C, s), 127.1, 126.3 (2C, s), 119.4, 114.8 (2C, s), 105.8, 102.0, 69.4. HRMS m/z [M+H]$^+$ calcd for $C_{21}H_{18}N_3O_2$: 344.1399 found = 344.1386; LC t_R = 4.33 min, >98% Purity.**4-{[4-(benzyloxy)phenyl]amino}quinazoline-6,7-diol** (**3**) as a light yellow solid (69 %, 189 mg, 0.527 mmol) MP 272-274 °C; ^{1}H NMR (400 MHz, DMSO-d_6) δ 10.32 (s, 2H), 8.53 (s, 1H), 7.91 (s, 1H), 7.64 – 7.53 (m, 2H), 7.50 – 7.44 (m, 2H), 7.43 – 7.37 (m, 2H), 7.36 – 7.30 (m, 2H), 7.20 (s, 1H), 7.10 – 7.01 (m, 2H), 5.13 (s, 2H). ^{13}C NMR (101 MHz, DMSO-d_6) δ 157.4, 155.7, 154.3, 149.1, 147.7, 137.1, 131.2, 128.5 (2C, s), 127.8, 127.7 (2C, s), 125.4 (2C, s), 114.7 (2C, s), 107.3, 106.7, 104.9, 69.4. HRMS m/z [M+H]$^+$ calcd for $C_{21}H_{18}N_3O_3$: 360.1348 found = 360.1335; LC t_R = 4.22 min, >98% Purity.***N*-(4-(benzyloxy)phenyl)-6-methoxyquinazolin-4-amine** (**4**) as a light yellow solid (84 %, 231 mg, 0.647 mmol) MP 270-272 °C; ^{1}H NMR (400 MHz, DMSO-d_6) δ 11.64 (s, 1H), 8.79 (s, 1H), 8.41 (d, *J* = 2.6Hz, 1H), 7.92 (d, *J* = 9.1 Hz, 1H), 7.72 (dd, *J* = 9.2, 2.5 Hz, 1H), 7.68 – 7.53 (m, 2H), 7.53 – 7.18 (m, 5H), 7.18 – 7.04 (m, 2H), 5.17 (s, 2H), 4.00 (s, 3H). ^{13}C NMR(101 MHz, DMSO-d_6) δ 159.0 (2C, s), 156.8, 148.8, 136.9, 133.3, 129.6, 128.5 (2C, s), 127.9, 127.7 (2C, s), 126.8, 126.4 (2C, s), 121.4, 114.9 (2C, s), 114.6, 104.6, 69.4, 56.7. HRMS m/z [M+H]$^+$ calcd for $C_{22}H_{19}N_3O_2$: 357.1477 found = 358.1546; LC t_R = 4.53 min, >98% Purity.***N*-[4-(benzyloxy)phenyl]-7-methoxyquinazolin-4-amine** (**5**) as a colourless solid (91 %, 251 mg, 0.701 mmol) MP 247-249 °C; ^{1}H NMR (400 MHz, DMSO-d_6) δ 11.58 (s, 1H), 8.87 (d, *J* = 9.3 Hz, 1H), 8.81 (s, 1H), 7.71 – 7.57 (m, 2H), 7.58 – 7.12 (m, 7H), 7.13 – 6.99 (m, 2H), 5.15 (s, 2H), 3.97 (s, 3H). ^{13}C NMR (101 MHz, DMSO-d_6) δ 164.7, 158.9, 156.7, 150.8, 140.7, 136.9, 129.6, 128.5 (2C, s), 127.9, 127.7 (2C, s), 127.0, 126.3 (2C, s), 118.7, 114.8 (2C, s), 107.1, 100.1, 69.4, 56.3. HRMS m/z [M+H]$^+$ calcd for $C_{22}H_{19}N_3O_2$: 357.1477 found = 358.1547; LC t_R = 4.49 min, >98% Purity.***N*-(4-(benzyloxy)phenyl)-6,7-dimethoxyquinazolin-4-amine** (**6**) as a colourless

solid (84 %, 217 mg, 0.561 mmol) MP 250-252 °C; ^{1}H NMR (400 MHz, DMSO-d_6) δ 11.44 (s, 1H), 8.73 (s, 1H), 8.36 (s, 1H), 7.68 – 7.56 (m, 2H), 7.55 – 7.43 (m, 2H), 7.43 – 7.15 (m, 4H), 7.15 – 7.03 (m, 2H), 5.15 (s, 2H), 4.00 (s, 3H), 3.96 (s, 3H). ^{13}C NMR (101 MHz, DMSO-d_6) δ 157.9, 156.5, 156.0, 150.0, 148.6, 137.0, 135.5, 129.9, 128.5 (2C, s), 127.9, 127.7 (2C, s), 126.3 (2C, s), 114.8 (2C, s), 107.1, 104.1, 99.8, 69.4, 57.0, 56.4. HRMS m/z [M+H]$^+$ calcd for $C_{23}H_{21}N_3O_3$: 388.1661 found = 388.1651; LC t_R = 4.55 min, >98% Purity. **4-{[4-(benzyloxy)phenyl]amino}quinolin-6-ol (7)** as a light yellow solid (64 %, 182 mg, 0.532 mmol) MP 218 – 220 °C; ^{1}H NMR (400 MHz, DMSO-d_6) δ 10.67 (s, 1H), 10.37 (s, 1H), 8.32 (d, J = 6.8 Hz, 1H), 7.96 (d, J = 9.1 Hz, 1H), 7.91 (d, J = 2.5 Hz, 1H), 7.63 (dd, J = 9.1, 2.4 Hz, 1H), 7.58 – 7.44 (m, 2H), 7.46 – 7.22 (m, 5H), 7.23 – 7.13 (m, 2H), 6.57 (d, J = 6.8 Hz, 1H), 5.17 (s, 2H). ^{13}C NMR(101 MHz, DMSO-d_6) δ 157.3, 156.5, 154.1, 140.1, 136.8, 132.2, 130.2, 128.5 (2C, s), 128.0, 127.8 (2C, s), 127.2 (2C, s), 124.9, 121.9, 118.7, 116.0 (2C, s), 105.4, 98.6, 69.5. HRMS m/z [M+H]$^+$ calcd for $C_{22}H_{19}N_2O_2$: 343.1447 found = 343.1433; LC t_R = 4.45 min, >98% Purity. **4-({4-[(4-fluorophenyl)methoxy]phenyl}amino)quinazolin-6-ol (8)** as a yellow solid (76 %, 228 mg, 0.631 mmol) Decomposed >200 °C; ^{1}H NMR (400 MHz, DMSO-d_6) δ 11.22 (s, 1H), 10.91 (s, 1H), 8.75 (s, 1H), 8.05 (d, J = 2.5 Hz, 1H), 7.88 (d, J = 9.0 Hz, 1H), 7.70 (dd, J = 9.0, 2.4 Hz, 1H), 7.67 – 7.54 (m, 2H), 7.57 – 7.39 (m, 2H), 7.40 – 7.17 (m, 2H), 7.17 – 7.01 (m, 2H), 5.14 (s, 2H). ^{13}C NMR (101 MHz, DMSO-d_6) δ 163.0, 159.7 (d, J = 175.5 Hz), 157.8, 156.6, 148.1, 133.2 (d, J = 3.0 Hz), 131.6, 130.0 (d, J = 8.3Hz, 2C), 129.8, 126.5, 126.2 (2C, s), 121.2 115.3 (d, J = 21.4 Hz, 2C), 114.93, 114.86 (2C, s), 107.1, 68.7. HRMS m/z [M+H]$^+$ calcd for $C_{21}H_{17}N_3O_2F$: 362.1305 found = 362.1290; LC t_R = 4.31 min, >98% Purity. **4-({4-[(3-fluorophenyl)methoxy]phenyl}amino)quinazolin-6-ol (9)** as a dark green solid (58 %, 174 mg, 0.482 mmol) 138 – 140 °C; ^{1}H NMR (400 MHz, DMSO-d_6) δ 11.25 (s, 1H), 10.94 (s, 1H), 8.74 (s, 1H), 8.06 (d, J = 2.5 Hz, 1H), 7.89 (d, J = 9.0 Hz, 1H), 7.71 (dd, J = 9.0, 2.4 Hz, 1H), 7.67 – 7.49 (m, 2H), 7.45 (td, J = 8.0, 6.0 Hz, 1H), 7.41 – 7.22 (m, 2H), 7.21 – 6.93 (m, 3H), 5.19 (s, 2H). ^{13}C NMR (101 MHz, DMSO-d_6) δ 162.20 (d, J = 243.7 Hz), 158.83, 157.80, 156.43, 148.07, 139.93 (d, J = 7.4 Hz), 131.62, 130.52 (d, J = 8.4 Hz), 129.89, 126.48, 126.26 (2C, s), 123.54 (d, J = 2.8 Hz), 121.14, 114.93, 114.87 (2C, s) , 114.63 (d, J = 20.9 Hz), 114.23 (d, J = 21.9 Hz), 107.13, 68.57 (d, J = 1.9 Hz). HRMS m/z [M+H]$^+$ calcd for $C_{21}H_{17}N_3O_2F$: 362.1305 found = 362.1296; LC t_R = 4.25 min, >98% Purity. **4-({4-[(2-fluorophenyl)methoxy]phenyl}amino)quinazolin-6-ol (10)** as a dark green solid (69 %, 207 mg, 0.573 mmol) 235 – 237 °C; ^{1}H NMR (400 MHz, DMSO-d_6) δ 11.23 (s, 1H), 10.91 (s, 1H), 8.75 (s, 1H), 8.05 (d, J = 2.5 Hz, 1H), 7.88 (d, J = 9.0 Hz, 1H), 7.70 (dd, J = 9.0, 2.4 Hz, 1H), 7.66 – 7.48 (m, 3H), 7.48 – 7.38 (m, 1H), 7.38 – 7.19 (m, 2H), 7.19 – 7.05 (m, 2H), 5.19 (s, 2H). ^{13}C NMR(101 MHz, DMSO-d_6) δ 160.4 (d, J = 246.1 Hz), 158.8, 157.8, 156.5, 148.1, 131.7, 130.7 (d, J = 4.1 Hz), 130.5 (d, J =8.3 Hz), 129.9, 126.5, 126.3 (2C, s), 124.6 (d, J = 3.5 Hz), 123.7 (d, J = 14.5 Hz), 121.2, 115.4 (d, J = 21.0 Hz), 114.9, 114.8 (2C, s), 107.1, 63.8 (d, J = 3.7 Hz). HRMS m/z [M+H]$^+$ calcd for $C_{21}H_{17}N_3O_2F$: 362.1305 found = 362.1291; LC t_R = 4.30 min, >98% Purity. **4-((4-((4-fluorobenzyl)oxy)phenyl)amino)quinazolin-7-ol (11)** as a grey solid (58 %, 174 mg, 0.482 mmol) Decomposed >300 °C; ^{1}H NMR (400 MHz, DMSO-d_6) δ 11.74 (s, 1H), 11.38 (s, 1H), 8.81 – 8.66 (m, 2H), 7.66 – 7.38 (m, 4H), 7.29 (dd, J = 6.9, 2.4 Hz, 2H), 7.27 – 7.15 (m, 2H), 7.14 – 7.5 (m, 2H), 5.13 (s, 2H). ^{13}C NMR (101 MHz, DMSO-d_6) δ 164.2, 161.8 (d, J = 243.7 Hz), 158.9, 156.5, 150.5, 140.5, 133.2 (d, J = 3.0 Hz), 130.0 (d, J = 8.3 Hz, 2C), 129.7, 127.1, 126.3 (2C, s), 119.4, 115.3 (d, J = 21.4 Hz, 2C), 114.8 (2C, s), 105.8, 102.1, 68.7. HRMS m/z [M+H]$^+$ calcd for $C_{21}H_{17}N_3O_2F$: 362.1305 found = 362.1291; LC t_R = 4.44 min, >98% Purity. **4-((4-((4-fluorobenzyl)oxy)phenyl)amino)quinazoline-6,7-diol (12)** as a colourless solid (55 %, 158 mg, 0.420 mmol) 285 – 290 °C; ^{1}H NMR (400 MHz, DMSO-d_6) δ 10.34 (s, 1H), 8.55 (s, 1H), 7.88 (s, 1H), 7.70 – 7.35 (m, 4H), 7.33 – 7.12 (m, 3H), 7.12 – 7.01 (m, 2H), 5.12(s, 2H). ^{13}C NMR(126 MHz, DMSO-d_6) δ 161.8 (d, J = 243.5 Hz), 157.4, 155.7, 154.4, 149.0, 147.7, 137.4, 133.3 (d, J = 8.3 Hz, 2C), 130.9, 130.0 (d, J = 8.4 Hz, 2C), 125.4, 115.3 (d, J = 21.3 Hz, 2C), 114.8 (s, 2C), 107.2, 106.8, 104.6, 68.7. HRMS m/z [M+H]$^+$ calcd for $C_{21}H_{17}N_3O_3F$: 378.1254 found = 378.1240; LC t_R = 4.29 min, >98% Purity.

15. Toxicity cell assay: WS-1 cells were seeded at 400 cells/well in 384 well plates. Cells were treated with compound at 24 h after plating, and cell viability was assessed at 48 h using alamarBlue (ThermoFisher, USA). Fluorescence was measured using Tecan Infinite 200 PRO plate reader with excitation at 535 nM and emission at 590 nM. IC_{50} values were determined by nonlinear regression using Graphpad PrismTM software.
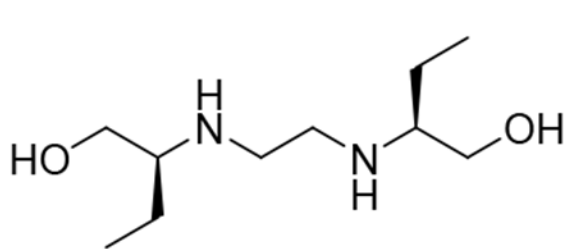
16. Compounds **13-28** prepared as previously described.[11]

17. Compounds **29-34** prepared as previously described.[18]

18. Asquith CRM; Maffuid KA; Laitinen T; Torrice CD; Tizzard GJ; Koshlap KM; Crona DJ; Zuercher WJ bioRxiv 2019, doi: 10.1101/545525
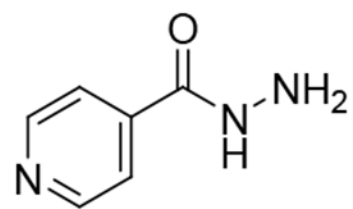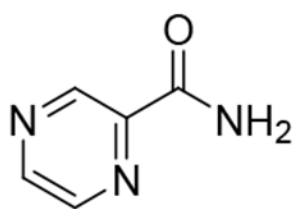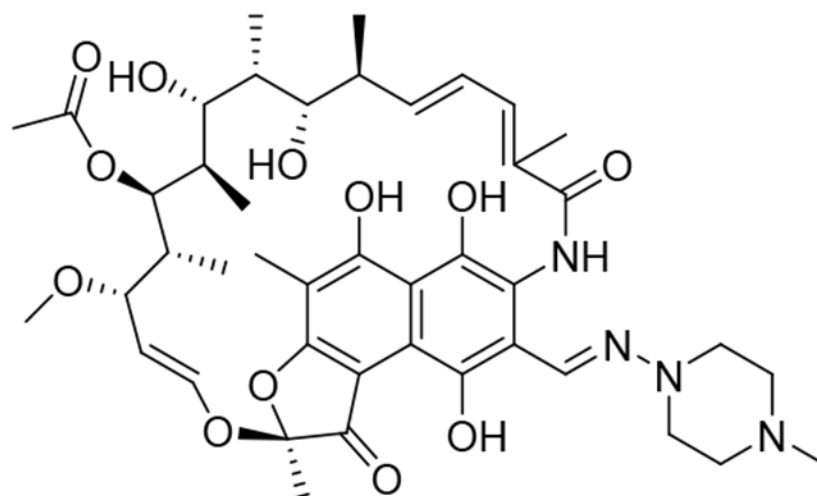
Figure 1.
Current therapeutic strategies for treatment of *Mycobacterium tuberculosis* infections.
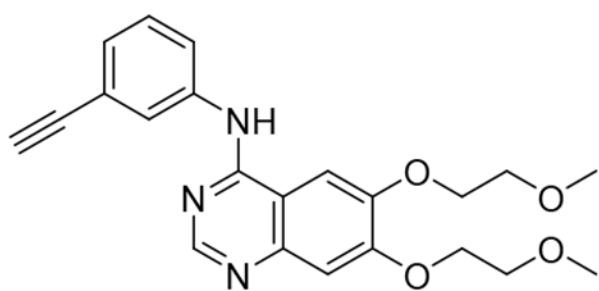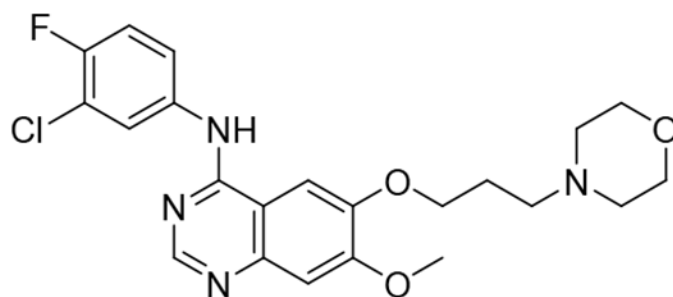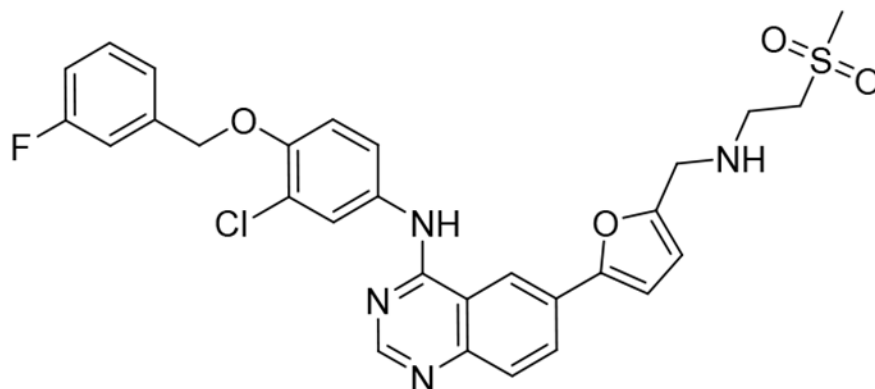
Figure 2.
Structures of clinical quinazolines.
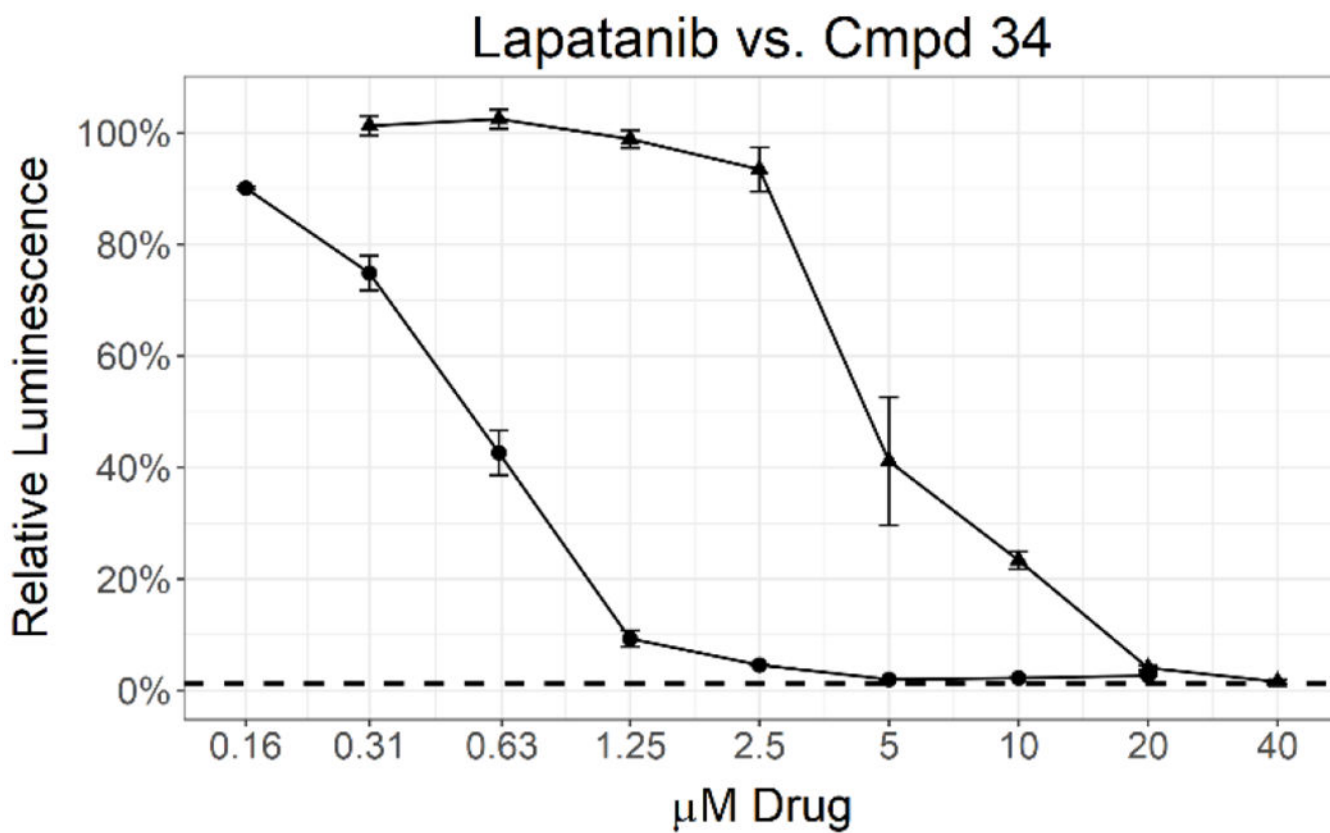
Figure 3.
MIC determination by two different assays for **34** (circle) and lapatanib (triangle). Data points represent the mean of 3 biological replicates with standard deviation. The dashed line labeled 1% inoculum represents an inoculation of 1 % of the number of cells used for compound testing. This control was used to determine 99 % inhibition of growth.

Scheme 1.
General synthetic procedure

Table 1.

Results of clinical inhibitors.

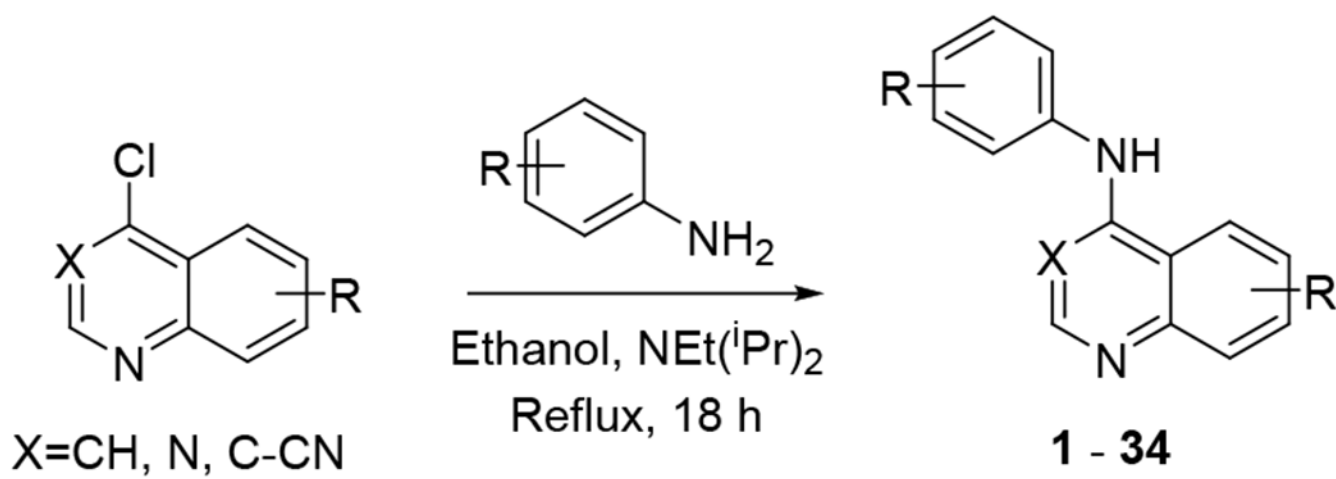| Compound/μM	*Mtb* signal[a]					WS-1[b]
	1.25	**2.5**	**5**	**10**	**20**	**(μM)**
Gefitinib	1.08	1.09	1.05	1.08	1.05	23
Erlotinib	1.05	0.96	0.9	0.68	0.7	8.6
Lapatinib	0.99	0.9	0.74	0.17	0.08	13

[a] Relative luminescence measured at 3 days after treatment. Values = RLU(sample)/RLU(no compound) at μM concentrations and no effect at 0.625 μM;

[b] ref11

Table 2.

Results of alcohol replacement of lapatinib and gefitinib (**1-12**).
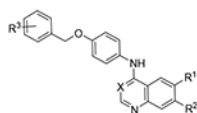
Compound	X	R^1	R^2	R^3	*Mtb* signal^a (μM)					WS-1^b
					1.25	**2.5**	**5**	**10**	**20**	**(μM)**
1	N	OH	H	H	0.95	0.94	0.96	0.90	0.80	26
2	N	H	OH	H	0.90	0.90	0.89	0.88	0.89	>100
3	N	OH	OH	H	0.95	0.93	0.91	0.76	0.69	8.8
4	N	OMe	H	H	1.04	1.07	0.89	0.83	0.62	>100
5	N	H	OMe	H	1.05	1.12	0.99	0.87	0.64	>100
6	N	OMe	OMe	H	1.04	1.04	0.83	0.77	0.6	>100
7	CH	OH	H	H	0.95	0.86	0.66	0.42	0.37	2.5
8	N	OH	H	4-F	0.86	0.76	0.64	0.44	0.32	>100
9	N	OH	H	3-F	0.76	0.64	0.49	0.39	0.25	12
10	N	OH	H	2-F	0.89	0.82	0.63	0.46	0.28	28
11	N	H	OH	4-F	0.94	1.01	0.90	0.89	0.83	>100
12	N	OH	OH	4-F	1.04	1.14	1.00	0.89	0.76	>100

^{a}Relative luminescence measured at 3 days after treatment. Values = RLU(sample)/RLU(no compound) at μM concentrations and no effect at 0.625 μM;

^{b}IC$_{50}$ (mean average n=4), 48 h

Table 3.

Matched pair comparison of structures similar to erlotinib and lapatinib (**13-28**).
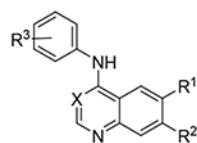
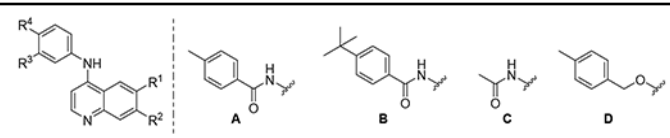| Compound	R^1	R^2	X	R^3	Mtb signal[a,b]			WS-1[c]
					5 μM	10 μM	20 μM	(μM)
13	CF$_3$	H	CH	3,4,5-(OMe)$_3$	1.23	1.14	1.21	>100
14	CF$_3$	H	N	3,4,5-(OMe)$_3$	1.25	1.12	1.06	>100
15	Br	H	CH	3,4,5-(OMe)$_3$	1.35	1.41	1.28	>100
16	OMe	OMe	CH	3,4,5-(OMe)$_3$	1.26	1.11	1.06	>100
17	OMe	OMe	N	3,4,5-(OMe)$_3$	1.03	1.01	0.94	>100
18	OMe	OMe	CN	3,4,5-(OMe)$_3$	1.03	1.01	0.97	>100
19	6,7-(OCH$_2$CH$_2$OMe)$_2$	N		3,4,5-(OMe)$_3$	1.02	0.96	0.87	>100
20	6,7-(OCH$_2$CH$_2$OMe)$_2$	CH		3-Ethynyl	0.88	0.79	0.58	>100
21	OMe	OMe	CH	3-Ethynyl	1.02	0.89	0.67	>100
22	OMe	OMe	N	3-Ethynyl	0.93	0.83	0.69	>100
23	OMe	OMe	CN	3-Ethynyl	1.08	1.03	0.98	>100
24	OMe	OMe	CH	3-Bromo	1.03	0.90	0.6	9.6
25	OMe	OMe	N	3-Bromo	0.98	0.71	0.65	3.9
26	OMe	OMe	CN	3-Bromo	0.88	0.56	0.37	11
27	OMe	OMe	N	3-Cl-4-(2-F-PhO)	0.92	0.74	0.80	1.1
28	OMe	OMe	CH	3-Cl-4-(2-F-PhO)	0.78	0.22	0.10	11

[a] Relative luminescence was measured at 3 days after treatment. Values = RLU(sample)/RLU(no compound);

[b] None of the compounds reduced the relative Mtb signal below 95 % at 1.3 or 2.5 μM;

[c] IC$_{50}$ (mean average n = 4), 48 h

Table 4.

Matched pair comparison of benzyloxyaniline.

Compound	R^1	R^2	R^3	R^4	*Mtb* signal[a] (μM)					WS-1[b]
					1.25	**2.5**	**5**	**10**	**20**	**(μM)**
29	OMe	OMe	OH	A	1.14	1.09	1.13	1.05	0.45	16
30	OMe	OMe	OH	B	1.10	1.12	1.06	0.72	0.25	2.6
31	OMe	OMe	H	C	1.21	1.10	1.11	1.07	1.02	9.7
32	OMe	H	OH	A	1.11	1.17	1.14	1.28	0.95	10
33	H	OMe	OH	A	1.13	1.11	1.09	1.11	0.96	4.7
34	OMe	OMe	H	D	0.43	0.17	0.10	0.08	0.09	5.4

[a] Relative luminescence was measured at 3 days after treatment. Values = RLU(sample)/RLU(no compound);

[b] IC$_{50}$ (mean average n=4), 48 h